Journal of Medicinal Chemistry

Brief Article

pubs.acs.org/jmc

Synthesis and Biological Characterization of 3-Substituted-1*H*-indoles as Ligands of GluN2B-Containing *N*-Methyl-D-aspartate Receptors

Rosaria Gitto,*[,†] Laura De Luca,[†] Stefania Ferro,[†] Maria Rosa Buemi,*[,†] Emilio Russo,[‡] Giovambattista De Sarro,[‡] Lara Costa,[§] Lucia Ciranna,[§] Orazio Prezzavento,[∥] Emanuela Arena,[∥] Simone Ronsisvalle,[∥] Giuseppe Bruno,[⊥] and Alba Chimirri[†]

[†]Dipartimento Farmaco-Chimico, Università di Messina, Viale Annunziata, I-98168 Messina, Italy

[‡]Dipartimento di Medicina Sperimentale e Clinica, Università Magna Græcia, Viale Europa Località Germaneto, I-88100 Catanzaro, Italy

[§]Dipartimento di Scienze Bio-Mediche, Sezione di Fisiologia, and [∥]Dipartimento di Scienze del Farmaco, Università di Catania, Viale Andrea Doria 6, I-95125 Catania, Italy

[⊥]Dipartimento di Chimica Inorganica, Chimica Analitica, e Chimica Fisica, Università di Messina, Salita Sperone 31, I-98100 Messina, Italy

Supporting Information

ABSTRACT: As an extension of our studies, novel indole derivatives were rationally designed and synthesized as ligands targeted to GluN2B/NMDA receptors. The 2-(4-benzylpiperidin-1-yl)-1-(6-hydroxy-1*H*-indol-3-yl)ethanone (**4i**) and 1-(4-benzylpiperidin-1-yl)-2-(6-hydroxy-1*H*-indol-3-yl)ethane-1,2-dione (**6i**) showed high binding affinity in [^{3}H]ifenprodil displacement assay. By computational studies, we suggested the hypothetical interactions playing a significant role during the binding process. However, in functional and in vivo studies the most potent compound **4i** did not show any activity whereas it displayed relevant affinity toward the σ_2 receptor.

INTRODUCTION

Glutamate NMDA receptors (NMDARs) are involved in many physiological processes such as neuronal development, learning, and memory but also in pathological states of mammalian central nervous system, including strokes, seizures, and pain.[1,2] NMDARs are multisubunit complexes containing GluN1, GluN2, and more rarely GluN3 subunits (formerly known as NR1−3).[3−5] The GluN2 subunit exists as four subtypes (GluN2A−D). They are organized into four modules containing (a) two large extracellular domains, the amino-terminal domain (ATD), and the agonist-binding domain (ABD), (b) three transmembrane segments (M1, M3, and M4) and a pore lining P-loop region (M2), and (c) an intracellular carboxy terminal domain (CTD). The ATD plays a key role in subunit assembly and exhibits a clamshell-like structure.[6] In the case of GluN2A and GluN2B subunits, the ATD binds allosteric inhibitors exerting modulator roles. Notably, the expression of GluN2B is restricted to forebrain areas and minimally in the cerebellum. This distribution implies that GluN2B selective antagonists might have reduced side effects in the treatment of neurological pathologies.[7−10] The prototypic noncompetitive GluN2B-antagonist ifenprodil (**1**, Chart 1), its more selective "prodil" analogue Ro 25-6981 (**2**), and some indole-2-carboxamides (e.g. **3**) have good potential as neuroprotective agents and have been described as GluN2B antagonists.[9,10] Recently it was demonstrated[11] that the GluN1 and GluN2B ATDs form a heterodimer; in particular, the crystal structures revealed that **1** and **2** bind at the interface between these two subunits rather than exclusively at the GluN2B-ATD cleft.[12−15]

Chart 1. GluN2B/NMDA Noncompetitive Antagonists

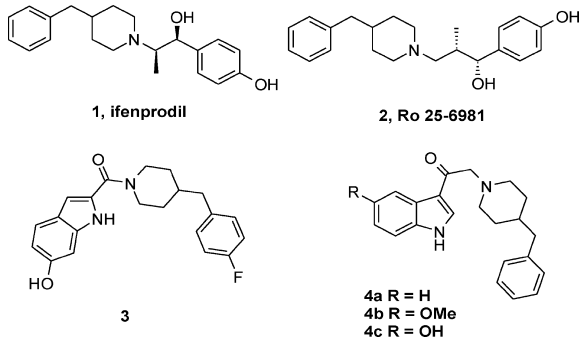

In previous studies we reported a molecular modeling strategy that led to the identification of some GluN2B ligands, containing indole scaffold,[16−18] structurally related to **3**. The most active derivatives **4a−c** (Chart 1) were able to prevent audiogenic seizures in DBA/2 mice, reduce NMDAR-mediated current in patch clamp experiments, and showed neuroprotective effects in HCN-1A cells.[16] Then structure−activity relationship (SAR) analysis highlighted some suitable structural requirements improving the recognition process for ifenprodil

Received: April 4, 2011
Published: November 3, 2011

Scheme 1[a]

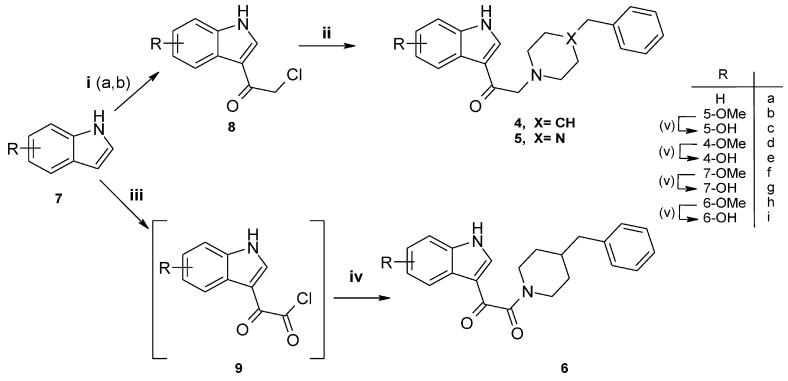

[a]Reagents and conditions: (i) (a) $ClCH_2COCl$, pyridine, dioxane, microwave (5 min, 50 °C, 200 W); (b) $ClCH_2CON(CH_3)_2$, $POCl_3$, room temp, 2.5 h; (ii) 4-benzylpiperidine or benzylpiperazine, K_2CO_3, DMF, microwave (10 min, 100 °C, 200 W); (iii) ClCOCOCl, diethyl ether, room temp, 2 h; (iv) 4-benzylpiperidine, THF, TEA, room temp, 2 h; (v) BBr_3 (1.0 M DCM), room temp, 10 h.

Table 1. GluN2B/NMDA Binding Affinities and Anticonvulsant Effects of Compounds 4−6

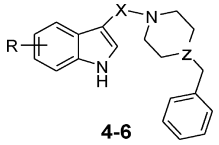

					ED_{50}, μmol/kg[b]	
compd	R	X	Z	% at 10 μM (IC_{50}, μM)[a]	clonus	tonus
4a	H	$COCH_2$	CH	89% (0.769)[c]	22.4 (13.9−36.2)[d]	8.71 (5.71−13.3)[d]
4b	5-OMe	$COCH_2$	CH	86%[d]	59.9 (38.7−92.7)[d]	36.5 (26.1−51.0)[d]
4c	5-OH	$COCH_2$	CH	92% (0.025)[c]	11.5 (7.96−16.5)[c]	6.48 (4.56−9.21)[c]
4d	4-OMe	$COCH_2$	CH	82% (0.324)	32.7 (20.0−53.6)	16.2(10.1−26.2)
4e	4-OH	$COCH_2$	CH	77% (6.64)	68.1(49.3−94.0)	13.7 (7.1−26.3)
4f	7-OMe	$COCH_2$	CH	62% (2.91)	80.3 (47.9−135)	35.8 (22.6−56.8)
4g	7-OH	$COCH_2$	CH	72% (7.14)	>100	53.8 (39.0−74.2)
4h	6-OMe	$COCH_2$	CH	4%	67.8 (45.9−100)	30.1 (20.8−43.4)
4i	6-OH	$COCH_2$	CH	92% (0.017)	95.4 (67.5−135)	53.7 (37.1−77.0)
5a	H	$COCH_2$	N	14%	>100[c]	>100[c]
5b	5-OMe	$COCH_2$	N	ND	98.7 (72.2−113)	63.8 (45.1−90.2)
5c	5-OH	$COCH_2$	N	27%	>100	44.9 (26.6−75.8)
6a	H	COCO	CH	36%[c]	22.4 (10.9−45.9)[c]	0.95 (0.26−3.52)[c]
6b	5-OMe	COCO	CH	9%	>100[c]	78.8 (53.7−116)[c]
6c	5-OH	COCO	CH	77% (2.66)[c]	>100[c]	>100[c]
6d	4-OMe	COCO	CH	14%	>100	76.7 (65.1−90.5)
6e	4-OH	COCO	CH	24%	52.1 (46.0−59.1)	28.9 (20.9−39.8)
6f	7-OMe	COCO	CH	33%	51.4 (38.5−68.6)	27.4 (18.8−39.9)
6g	7-OH	COCO	CH	79% (1.99)	80.5 (59.4−109)	36.2 (23.0−57.1)
6h	6-OMe	COCO	CH	ND	11.9 (8.97−15.9)	4.68 (3.02−7.25)
6i	6-OH	COCO	CH	92% (0.022)	84.4 (56.3−126)	38.9 (25.1−60.5)

[a]Displacement of [^{3}H]ifenprodil. ND = not detectable. [b]All data were calculated following the Litchfield and Wilcoxon method. At least 32 animals were used to calculate each ED_{50}. 95% confidence limits are given in parentheses. [c]Reference 18. [d]Reference 16

site.[18] In an attempt to confirm these results and further explore the hypothetical binding interactions, we designed novel ligands. (i) We prepared derivatives bearing methoxy or hydroxyl groups in the 4, 5, 6, or 7 position of indole skeleton. (ii) We went thoroughly into the influence of a positive ionizable feature of the piperidine nitrogen atom, introducing an oxalyl group as linker and, on the basis of experimental evidence, suggesting that there is a significant reduction of side effects for GluN2B antagonists lacking a basic nitrogen (e.g., **3**). (iii) We also substituted the benzylpiperidine fragment with a benzylpiperazine one, thus offering the possibility of an alternative anchoring point for the electrostatic interaction by nitrogen atom. We evaluated the effects of the structural modifications on binding affinity, anticonvulsant properties, and functional activity in patch-clamp experiments. Moreover, docking simulations were carried out to explain the obtained biological results, taking into account the recent findings concerning the NMDAR subunit arrangement.[11] Finally, the σ_1/σ_2 receptor binding affinities of selected indoles were evaluated in an attempt to clarify some biological results.

dx.doi.org/10.1021/jm2008002 | J. Med. Chem. 2011, 54, 8702−8706

CHEMISTRY

The synthetic pathways are depicted in Scheme 1. We synthesized 2-chloro-1-(1*H*-indol-3-yl)ethanone derivatives **8** following our previously reported method (pathway a)[18] or an optimized strategy (pathway b), thus improving the yields and obtaining a cleaner reaction. Starting from intermediates **8**, the corresponding 2-(4-benzylpiperidin-1-yl)-1-(1*H*-indol-3-yl)-ethanones (**4**) and 2-(4-benzylpiperazin-1-yl)-1-(1*H*-indol-3-yl)ethanones **5** were obtained. In a similar way we prepared the 1-(4-benzylpiperidin-1-yl)-2-(1*H*-indol-3-yl)ethane-1,2-diones (**6**) through 2-(1*H*-indol-3-yl)-2-oxoacetyl chloride intermediates (**9**). All methoxyindole derivatives were readily converted into the hydroxy analogues upon treatment with boron tribromide. The chemical characterization of new compounds obtained was supported by elemental analyses and spectroscopic measurements (see Supporting Information).

RESULTS AND DISCUSSION

To further study the SARs of this series of novel indole derivatives (**4d−i**, **5b,c**, **6d−i**), we evaluated their ability to interact with the GluN2B subunit by testing [^{3}H]ifenprodil binding inhibition and the results were compared with those of previously reported **4−6** analogues and ifenprodil (**1**) (Table 1).[16,18] The 2-(4-benzylpiperidin-1-yl)-1-(6-hydroxy-1*H*-indol-3-yl)ethanone (**4i**), displaying the highest binding affinity (IC_{50} = 0.017 μM), showed a 45-fold improvement over the unsubstituted parent **4a** and a potency comparable to that of the 5-hydroxy analogue **4c** and ifenprodil (**1**) (IC_{50} = 0.020 μM). In contrast, the introduction of a 6-methoxy substituent (e.g., **4h**) led to a reduction of [^{3}H]ifenprodil displacement. Also, the replacement of benzylpiperidine with benzylpiperazine fragment reduced the affinity of **5a−c** in comparison with **4a−c**. The oxalyl analogues **6a−h** generally demonstrated a significant decrease in GluN2B affinity with respect to **4a−h**; however, for **6c** and **6g** we observed moderate inhibition properties (IC_{50} of 2.66 and 1.99 μM, respectively). Unexpectedly, **6i** was extraordinarily efficacious displaying IC_{50} comparable to those of **4c** and **1**. Overall, the lowest IC_{50} values were obtained for compounds containing a 5- or 6-hydroxyl substituent on benzene fused ring, whereas the substitution at the 4- or 7-position led to less active ligands **4e** and **4g**, and generally the optimization of affinity seems to reside in the positive ionizable feature of piperidine nitrogen atom.

To rationalize the obtained biological data, docking simulations by Gold (see Supporting Information) were performed using the structural coordinates (PDB code 3QEL) for the heterodimer GluN1b-GluN2B in complex with ifenprodil (**1**). First, test docking calculations using **1** and Ro 25-6981 (**2**) were carried out to compare experimental and predicted binding modes and to validate our docking protocol. The best **1** and **2** docking poses agreed well with the experimental binding modes with rmsd of 0.6 and 0.65, respectively. Figure 1A displays the superposition of the indoles **4c** (magenta) and **4i** (orange). They present a very similar binding mode in the GluN1b-GluN2B subunit interface in accordance with their comparable binding affinities (IC_{50} of 25 and 17 nM, respectively). We found hydrogen bonding interactions between the hydroxyl group at C-5 (for **4c**) or C-6 (for **4i**) and residue E236 of GluN2B and between residue K131 of GluN1b and NH of indole ring. Furthermore, through the protonated piperidine nitrogen atom, **4c** and **4i** make polar

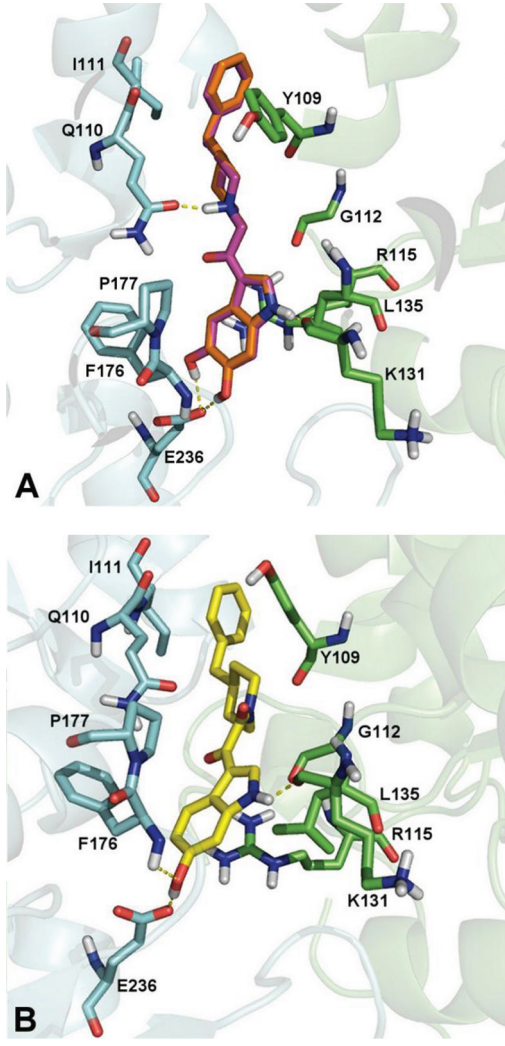

Figure 1. Docking poses of **4c**, **4i**, and **6i** at the GluN1b-Glun2B subunit interface: (A) binding of **4c** (magenta) compared to **4i** (orange); (B) binding of **6i** (yellow). Important residues are drawn in stick and colored in cyan (GluN2B) and in green (GluN1b). Hydrogen bonds (shown as dashed yellow lines) are formed between the compounds and GluN1b-Glun2B subunit interface. The structures were prepared using PyMOL.[28]

interactions with residue Q110 of GluN2B. Finally, they form interactions with hydrophobic portions of some residues on GluN1b (Y109, G112, L135) and GluN2B (I111, F176, P177). Notably, our docking results are in good agreement with the interactions highlighted in the crystal structures of the GluN1b-GluN2B ATD heterodimer in complex with ifenprodil (**1**) and Ro 25-6981 (**2**).[11] In particular, the major contacts of **1** and **2** were (i) polar interactions of the hydroxylphenyl group with E236 residue and the positive ionizable nitrogen atom with Q110 residue and (ii) hydrophobic interactions mediated by L135 residue on GluN1b subunit and F176 and P177 residues on the GluN2B subunit.

Considering that **4a−h** generally showed lower IC_{50} with respect to **6a−h**, we chose to study the correlation between the binding affinities and piperidine nitrogen atom basicity. The gas phase proton affinity (PA) of **4c** and **6c** has been calculated. As expected in the case of 2-(4-benzylpiperidin-1-yl)-1-(5-hydroxy-1*H*-indol-3-yl)ethanone (**4c**, −243,18 kcal/mol) the PA value was higher than that of the corresponding oxalyl

dx.doi.org/10.1021/jm2008002 | *J. Med. Chem.* 2011, 54, 8702−8706

analogue (**6c**, −217.43 kcal/mol). Combining the docking results and PA calculations, we suggested a key role of the interaction between ionizable nitrogen atom and residue Q110, thus generally justifying the different affinity between compound types **4** and **6**. Unexpectedly, the 6-hydroxy derivative **6i** showed a low IC_{50} (0.022 μM) with respect other **6** analogues. So we docked **6i** in the GluN1b-GluN2B subunit interface (see Figure 1B). We found that **6i** assumes a binding mode similar to those of **4c** and **4i** except for polar contact with Q110; however, we observed strong contacts with hydrophobic residues of GluN1b subunit such as Y109, G112, and L135. These last interactions could provide a reasonable explanation for the high binding affinity of **6i** even if it lacks a positive ionizable feature.

To investigate the functional activity of **4i**, we have tested its effect on NMDA-mediated current in CA1 pyramidal neurons from mouse hippocampal slices using whole-cell patch clamp. Application of NMDA (50 μM, 2 s) in the presence of glycine (0.5 μM) and tetrodotoxin (TTX, 0.5 μM) induced an inward current with a mean amplitude of 507 ± 115 pA (mean ± SEM, n = 7, range 251−1115 pA in different neurons, median 371 pA). In the presence of **4i** (10 μM, 5 min) the amplitude of NMDA-mediated current was not significantly different from control (Figure 2; P = 0.27, t test, n = 7). Figure 2 illustrates

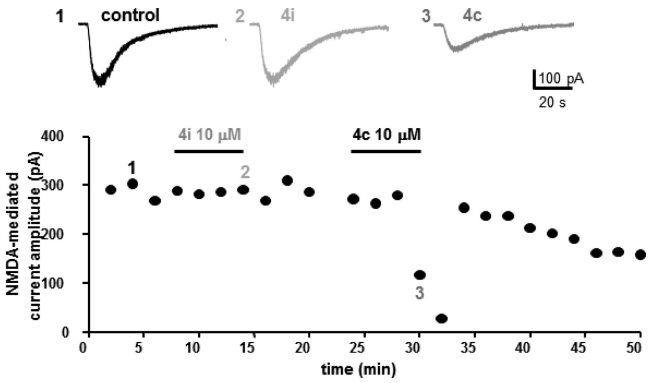

Figure 2. Application of NMDA (50 μM, 2 s) induced an inward current (trace 1) that was not modified during simultaneous application of compound **4i** (10 μM, 5 min, trace 2) but was significantly reduced by **4c** (10 μM, 5 min, trace 3), a selective antagonist of GluN2B receptors. NMDA current amplitude values (pA) were represented on a graphic as a function of time to illustrate the time course of effects.

representative traces from a neuron in which NMDA current amplitude was not modified by **4i** but was significantly reduced by **4c** (P < 0.01, t test, n = 7, see Supporting Information) previously characterized as a GluN2B antagonist.[18] These results indicate that in spite of its high binding affinity, **4i** did not significantly antagonize NMDA-mediated effect. To explain the different results observed for **4c** and **4i**, we turned our attention to the possibility that our indoles could exert some off-target activities. So we evaluated the binding affinity toward σ receptors on the basis of the following assumptions: (i) ifenprodil (**1**) and its analogues also bind σ_1 and σ_2 receptors;[19,20] (ii) presynaptic σ receptors were shown to modulate hippocampal glutamate release;[21,22] (iii) activation of σ receptors also modulates NMDA-mediated transmission.[23,24] Furthermore, molecules containing benzylpiperidine or benzylpiperazine fragment bind σ_1 and σ_2 receptors.[25,26] To determine affinities at σ_1 and σ_2 receptors, some selected hydroxyindole derivatives **4c**, **4i**, **5c**, **6c**, and **6i** and reference compounds **1** and **2** were subjected to binding testing. Competitive displacement of [^{3}H](+)pentazocine and [^{3}H]DTG [1,3-di-*o*-tolylguanidine] in the presence of (+)-SKF10,047 (0.4 μM) was used to determine σ_1 and σ_2 receptor affinities. The measured K_i revealed that **4c**, **4i**, **6c**, and **6i** had practically no affinity for σ_1 receptor (K_i > 1000). The *N*-benzylpiperazine derivative **5c** displayed moderate affinity at both σ receptors (K_i of 437 and 557 nM, respectively). Interestingly, **4c** and **4i** showed nanomolar σ_2 affinity (K_i of 76.5 and 43.0 nM, respectively) and a relevant selectivity over σ_1 subtype ($K_i(\sigma_1)/K_i(\sigma_2)$ > 60) when compared with **1** and **2** (see Supporting Information). Therefore, we can speculate that the effects exerted by **4i** on NMDA-mediated current (Figure 2) might be due to the interaction with GluN2B site and σ_2 receptor, whereas we cannot explain the biological profile of **4c**. However, we are currently investigating if each of these two compounds behaves as agonist or antagonist of the σ_2 receptor.

We also examined the anticonvulsant properties of all synthesized compounds against audiogenic seizures in DBA/2 mice.[27] The results were compared with those of the previously reported analogues **4a−c**, **5a**, **6a−c** (Table 1) and **2** (ED_{50} = 40.0 μmol/kg in clonic phase).[18] The obtained data indicated that there is no clear correlation between the binding results and in vivo data. Disappointingly, the most in vivo potent indole derivatives **4d**, **6a**, and **6h** did not show any significant [^{3}H]ifenprodil displacement properties. In contrast, for **4i** we found an excellent binding affinity but low anticonvulsant efficacy, in agreement with its effects on NMDA-induced currents.

■ CONCLUSIONS

We identified new hydroxylindoles as potent GluN2B ligands showing affinity similar to that of the ifenprodil (**1**). By means of docking studies based on recently published findings[11] about the arrangement of GluN1b-GluN2B NMDA receptors, we suggested the hypothetic binding orientation of the most interesting compounds **4c**, **4i**, and **6i** in the ifenprodil binding site. This investigation also gave information concerning similarities and differences in the binding modes of the synthesized compounds due to the presence/absence of positive ionizable nitrogen atom. Different from reference compounds **1** and **2**, the indole derivatives **4c** and **4i** were potent and selective σ_2 ligands. Further studies are in progress to clarify if the unexpected behavior of **4i** in functional and in in vivo studies could be connected (i) to its ability to exert some off-target activities or (ii) to its pharmacokinetic properties influencing the brain penetration.

■ EXPERIMENTAL SECTION

Chemistry. All starting materials and reagents commercially available (Sigma-Aldrich, Milan, Italy) were used without further purification. Microwave-assisted reactions were carried out in a CEM focused microwave synthesis system. Melting points were determined on a Stuart SMP10 apparatus and are uncorrected. By combustion analysis (C, H, N) carried out on a Carlo Erba model 1106 elemental analyzer, we determined the purity of synthesized compounds; the results confirmed a ≥95% purity. ^{1}H NMR spectra were measured in $CDCl_3$ or dimethylsulfoxide-d_6 (DMSO-d_6) with a Varian Gemini 300 spectrometer; chemical shifts are expressed in δ (ppm) and coupling constants (J) in Hz. All exchangeable protons were confirmed by addition of D_2O.

Synthesis of 2-(4-Benzylpiperidin-1-yl)-1-(1*H*-indol-3-yl)-ethanones (4d,f,h), 2-(4-Benzylpiperazin-1-yl)-1-(1*H*-indol-3-

dx.doi.org/10.1021/jm2008002 | J. Med. Chem. 2011, 54, 8702−8706

yl)ethanone (5b), and 1-(4-Benzylpiperidin-1-yl)-2-(1*H*-indol-3-yl)ethane-1,2-diones (6d,f,h). The appropriate 3-chloroacetylindole derivatives (**8b,d,f,h**) (1 mmol), benzylpiperidine (0.176 mL, 1 mmol) or benzylpiperazine (176.3 mg, 1 mmol), and K_2CO_3 (147.1 mg, 0.5 mmol) in DMF (2 mL) were stirred and irradiated in a microwave oven under the following conditions: 10 min, 100 °C, 200 W. The reaction mixture was quenched with $NaHCO_3$ saturated aqueous solution (10 mL) and extracted with ethyl acetate (3 × 10 mL). The organic phases were dried over dry Na_2SO_4. After removal of the solvent under reduced pressure, the residue was crystallized from ethanol to give desired **4** and **5**. The appropriate indole derivatives **7d,f,h** (1 mmol) were used as starting material to synthesize **6d,f,h** following a previously reported procedure.[18]

Starting from methoxy substituted derivatives **4d,f,h**, **5b**, and **6d,f,h**, the corresponding hydroxyl derivatives **4e,g,i**, **5c**, and **6e,g,i** were prepared using a previously published procedure.[18] Detailed analytical data of all new synthesized compounds are in the Supporting Information.

■ ASSOCIATED CONTENT

Ⓢ Supporting Information

Details for synthetic procedures and spectral data, assay protocols, dose−response curves, binding affinity data, and modeling parameters. This material is available free of charge via the Internet at http://pubs.acs.org.

■ AUTHOR INFORMATION

Corresponding Author

*For R.G.: phone, 00390906766413; fax, 00390906766402; e-mail, rgitto@unime.it. For M.R.B.: phone, 00390906766465; e-mail, mbuemi@unime.it.

■ ACKNOWLEDGMENTS

Financial support for this research by MiUR (Prin2008, Grant No. 20085HR5JK_002) is gratefully acknowledged.

■ ABBREVIATIONS USED

ABD, agonist-binding domain; CTD, carboxy terminal domain; DBA, dilute brown, nonagouti; iGluR, ionotropic glutamate receptor; HCN-1A, human cortical neuron 1A cell line; NMDA, *N*-methyl-D-aspartate; NMDAR, *N*-methyl-D-aspartate receptor; ATD, amino-terminal domain; PA, proton affinity; rmsd, root mean square deviation; TTX, tetrodotoxin

■ REFERENCES

(1) Paoletti, P. Molecular basis of NMDA receptor functional diversity. *Eur. J. Neurosci.* **2011**, *33*, 1351−1365.
(2) Muir, K. W. Glutamate-based therapeutic approaches: clinical trials with NMDA antagonists. *Curr. Opin. Pharmacol.* **2006**, *6*, 53−60.
(3) Traynelis, S. F.; Wollmuth, L. P.; McBain, C. J.; Menniti, F. S.; Vance, K. M.; Ogden, K. K.; Hansen, K. B.; Yuan, H.; Myers, S. J.; Dingledine, R. Glutamate receptor ion channels: structure, regulation, and function. *Pharmacol. Rev.* **2010**, *62*, 405−96.
(4) Paoletti, P.; Neyton, J. NMDA receptor subunits: function and pharmacology. *Curr. Opin. Pharmacol.* **2007**, *7*, 39−47.
(5) Collingridge, G. L.; Olsen, R. W.; Peters, J.; Spedding, M. A nomenclature for ligand-gated ion channels. *Neuropharmacology* **2009**, *56*, 2−5.
(6) Gielen, M.; Siegler Retchless, B.; Mony, L.; Johnson, J. W.; Paoletti, P. Mechanism of differential control of NMDA receptor activity by NR2 subunits. *Nature* **2009**, *459*, 703−707.
(7) Kohr, G. NMDA receptor antagonists: tools in neuroscience with promise for treating CNS pathologies. *J. Physiol. (London)* **2007**, *581*, 1−2.
(8) Gogas, K. R. Glutamate-based therapeutic approaches: NR2B receptor antagonists. *Curr. Opin. Pharmacol.* **2006**, *6*, 68−74.
(9) Borza, I.; Domany, G. NR2B selective NMDA antagonists: the evolution of the ifenprodil-type pharmacophore. *Curr. Top. Med. Chem.* **2006**, *6*, 687−695.
(10) Mony, L.; Kew, J. N.; Gunthorpe, M. J.; Paoletti, P. Allosteric modulators of NR2B-containing NMDA receptors: molecular mechanisms and therapeutic potential. *Br. J. Pharmacol.* **2009**, *157*, 1301−1317.
(11) Karakas, E.; Simorowski, N.; Furukawa, H. Subunit arrangement and phenylethanolamine binding in GluN1/GluN2B NMDA receptors. *Nature* **2011**, *475*, 249−253.
(12) Beinat, C.; Banister, S.; Moussa, I.; Reynolds, A. J.; McErlean, C. S.; Kassiou, M. Insights into structure−activity relationships and CNS therapeutic applications of NR2B selective antagonists. *Curr. Med. Chem.* **2010**, *17*, 4166−4190.
(13) Mony, L.; Krzaczkowski, L.; Leonetti, M.; Le Goff, A.; Alarcon, K.; Neyton, J.; Bertrand, H. O.; Acher, F.; Paoletti, P. Structural basis of NR2B-selective antagonist recognition by *N*-methyl-D-aspartate receptors. *Mol. Pharmacol.* **2009**, *75*, 60−74.
(14) McCauley, J. A. NR2B subtype-selective NMDA receptor antagonists: 2001−2004. *Expert Opin. Ther. Pat.* **2005**, *15*, 389−407.
(15) Nikam, S. S.; Meltzer, L. T. NR2B selective NMDA receptor antagonists. *Curr. Pharm. Des.* **2002**, *8*, 845−855.
(16) Gitto, R.; De Luca, L.; Ferro, S.; Occhiuto, F.; Samperi, S.; De Sarro, G.; Russo, E.; Ciranna, L.; Costa, L.; Chimirri, A. Computational studies to discover a new NR2B/NMDA receptor antagonist and evaluation of pharmacological profile. *ChemMedChem* **2008**, *3*, 1539−1548.
(17) Chimirri, A.; De Luca, L.; Ferro, S.; De Sarro, G.; Ciranna, L.; Gitto, R. Combined strategies for the discovery of ionotropic glutamate receptor antagonists. *ChemMedChem* **2009**, *4*, 917−922.
(18) Gitto, R.; De Luca, L.; Ferro, S.; Citraro, R.; De Sarro, G.; Costa, L.; Ciranna, L.; Chimirri, A. Development of 3-substituted-1*H*-indole derivatives as NR2B/NMDA receptor antagonists. *Bioorg. Med. Chem.* **2009**, *17*, 1640−1647.
(19) Antonini, V.; Prezzavento, O.; Coradazzi, M.; Marrazzo, A.; Ronsisvalle, S.; Arena, E.; Leanza, G. Anti-amnesic properties of (+/−)-PPCC, a novel sigma receptor ligand, on cognitive dysfunction induced by selective cholinergic lesion in rats. *J. Neurochem.* **2009**, *109*, 744−754.
(20) Tewes, B.; Frehland, B.; Schepmann, D.; Schmidtke, K. U.; Winckler, T.; Wunsch, B. Design, synthesis, and biological evaluation of 3-benzazepin-1-ols as NR2B-selective NMDA receptor antagonists. *ChemMedChem* **2010**, *5*, 687−695.
(21) Cobos, E. J.; Entrena, J. M.; Nieto, F. R.; Cendan, C. M.; Del Pozo, E. Pharmacology and therapeutic potential of sigma(1) receptor ligands. *Curr. Neuropharmacol.* **2008**, *6*, 344−366.
(22) Maurice, T.; Su, T. P. The pharmacology of sigma-1 receptors. *Pharmacol. Ther.* **2009**, *124*, 195−206.
(23) Monnet, F. P.; Debonnel, G.; Junien, J. L.; De Montigny, C. *N*-Methyl-D-aspartate-induced neuronal activation is selectively modulated by sigma receptors. *Eur. J. Pharmacol.* **1990**, *179*, 441−445.
(24) Martina, M.; Turcotte, M. E.; Halman, S.; Bergeron, R. The sigma-1 receptor modulates NMDA receptor synaptic transmission and plasticity via SK channels in rat hippocampus. *J. Physiol.* **2007**, *578*, 143−157.
(25) Moussa, I. A.; Banister, S. D.; Beinat, C.; Giboureau, N.; Reynolds, A. J.; Kassiou, M. Design, synthesis, and structure−affinity relationships of regioisomeric *N*-benzyl alkyl ether piperazine derivatives as sigma-1 receptor ligands. *J. Med. Chem.* **2010**, *53*, 6228−6239.
(26) Glennon, R. A. Pharmacophore identification for sigma-1 (sigma1) receptor binding: application of the "deconstruction−reconstruction−elaboration" approach. *Mini-Rev. Med. Chem.* **2005**, *5*, 927−940.
(27) Chapman, A. G.; Croucher, M. J.; Meldrum, B. S. Evaluation of anticonvulsant drugs in DBA/2 mice with sound-induced seizures. *Arzneim. Forsch.* **1984**, *34*, 1261−1264.
(28) Delano, W. L. *The PyMOL Molecular Graphics System*, version 0.99; Schrodinger LLC: San Francisco, CA, 2006.